



Time-resolved studies on correlations between dynamic electronic structure and selectivity of a $\text{H}_5[\text{PV}_2\text{Mo}_{10}\text{O}_{40}]$ partial oxidation catalyst

T. Ressler*¹, O. Timpe²

¹Technical University Berlin, Institute of Chemistry, Sekr. C 2, Strasse des 17 Juni 135, D-10623 Berlin, Germany

²Department of Inorganic Chemistry, Fritz-Haber-Institute of the MPG, Faradayweg 4-6, 14195 Berlin, Germany

* Corresponding author: e-mail Thorsten.Ressler@TU-berlin.de, Phone: +49 (0) 30 314 79736, Fax: +49 0 30 314 21106

Received 25 August 2006; revised 10 January 2007; accepted 22 January 2007. Available online 8 March 2007

Abstract

Time-resolved in situ X-ray absorption spectroscopy studies on an activated $\text{H}_5[\text{PV}_2\text{Mo}_{10}\text{O}_{40}]$ oxidation catalyst were performed to obtain correlations between the dynamic structure and the catalytic selectivity of the material. Both the geometric and the electronic structure of the vanadium and molybdenum metal centers of the catalyst change dynamically under the reaction conditions employed. Moreover, the selectivity of the catalyst exhibited a pronounced correlation with the degree of reduction and the solid-state kinetics of the re-oxidation process. The corresponding extent of re-oxidation curve could be simulated with a solid-state kinetic model assuming three-dimensional diffusion as rate-limiting step. Hence, the partially reduced catalyst exhibited a rate constant of the bulk-diffusion limited re-oxidation, which coincided with the temporal evolution of the selectivity of the catalyst.

Keywords: In situ, heterogeneous catalysis, structure-activity relationships, molybdenum, vanadium, EXAFS spectroscopy, polyoxometalates, time-resolution, dynamic, solid-state kinetics

Introduction

In situ studies on heterogeneous catalysts are indispensable in modern catalysis research. Reliable correlations between the structure of the catalyst and its catalytic performance can only be determined under relevant reaction conditions. These correlations need to be elucidated because they constitute the foundation of a knowledge-based design of novel heterogeneous catalysts. [1] Hence, many structural analytic techniques including X-ray absorption spectroscopy (XAS) have been used to study the bulk or surface structure of a catalyst under reaction conditions. [6] However, investigating a solid heterogeneous catalyst under steady-state reaction conditions yields little information on the dynamic nature of its surface and bulk structure. Heterogeneous catalysts are metastable materials whose structure and performance change dynamically under reaction conditions. Therefore, time-resolved measurements are required to further elucidate the behavior of the electronic and geometric structure of a catalyst under changing reaction conditions. Monitoring the gas phase composition during a catalytic reaction yields conventional kinetic in-

formation. Conversely, monitoring bulk structural changes reveals the solid-state kinetics of dynamic structural changes in the bulk of the catalyst under reaction conditions. In combination with simultaneous activity and selectivity measurements by suitable gas phase analytical techniques, the desired correlations between the catalytic performance and the bulk structure dynamics are obtained.

Heteropolyoxomolybdates of the Keggin type (e.g. $\text{H}_3[\text{PMo}_{12}\text{O}_{40}]$) are active catalysts for the partial oxidation of alkanes and alkenes. [8-12] Because of their molecular structure, heteropolyoxomolybdates of the Keggin type have been frequently employed as suitable model systems for more complex molybdenum based mixed oxide catalysts. However, the "real structure" of the Keggin ion under reaction conditions is not necessarily identical to the ideal structure of the corresponding as-prepared heteropolyoxomolybdate. In addition to the "ideal (crystallographic) structure", the "real structure" comprises all deviations from the ideal structure which may be present in the bulk structure of the catalyst. We have recently shown, that the onset of catalytic activity during thermal activation of $\text{H}_3[\text{PMo}_{12}\text{O}_{40}] * 13 \text{H}_2\text{O}$ and $\text{H}_4[\text{PVMo}_{11}\text{O}_{40}] * 13 \text{H}_2\text{O}$ in

propene coincides with a partial decomposition of the Keggin ion at ~ 600 K and migration of Mo centers on extra-Keggin sites. [13,14] Here, we report on correlations between the electronic structure and the catalytic selectivity of $H_5[PV_2Mo_{10}O_{40}] \cdot 13 H_2O$ under steady-state and dynamic reaction conditions obtained from time-resolved in situ XAS investigations.

Experimental

Preparation of $H_5[PV_2Mo_{10}O_{40}] \cdot 13 H_2O$

16.89 g of MoO_3 (corresponding to 11.73 mmol Mo_{10}) and 2.134 g of V_2O_5 (corresponding to 11.73 mmol V_2) were suspended in 650 ml water in a three-necked 1000 ml flask equipped with a condenser. Commercial phosphoric acid (H_3PO_4 ($\sim 82.5\%$)) was diluted by a factor of 100 and the exact concentration was determined by titration with NaOH. 81 ml of this 0.825 % H_3PO_4 solution (11.73 mmol P) were added dropwise to the boiling and stirred suspension of the metal oxides. After complete addition of the phosphoric acid a clear amber colored solution was obtained. The solid product was isolated by removing the solvent in a rotary evaporator at ~ 90 °C and dried in a vacuum desiccator. [15,16] Thermal analysis studies (TG/DTA-MS) confirmed the amount of ~ 13 molecules „crystal water“ per Keggin ion in as-prepared $H_5[PV_2Mo_{10}O_{40}] \cdot 13 H_2O$ and a similar thermal stability as $H_4[PVMo_{11}O_{40}] \cdot 13 H_2O$.

X-ray diffraction (XRD)

XRD measurements were performed on a *STOE STADI P* diffractometer (Cu $K\alpha_1$; Ge primary monochromator) in a range of $5^\circ - 100^\circ$ in 2θ with a step width of 0.01° and a measuring time of 10 sec/step. Structural refinements to the experimental diffraction patterns were performed using the software TOPAS v 2.1 (Bruker AXS). Structural data employed in the XRD and XAS analyses were taken from the Inorganic Crystal Structure Database (ICSD).

X-ray absorption spectroscopy (XAS)

In situ transmission XAS experiments were performed at the V K edge (5.465 keV, Si 111) and at the Mo K edge (19.999 keV, Si 311) at beamlines E4 and X1, respectively, at the *Hamburg Synchrotron Radiation Laboratory*, HASYLAB. The storage ring operated at 4.4 GeV with injection currents of 150 mA. The in situ experiments were conducted in a flow-reactor at 1 bar in flowing reactants (flow rate of 30 ml/min, heating rate of 5 K/min to the reaction temperatures employed). The gas phase composition at the cell outlet was continuously analyzed using a non-calibrated mass spectrometer in a multiple ion detection mode (Omnistar from Pfeiffer).

The heteropolyoxomolybdate was mixed with boron nitride (~ 7 mg HPOM and ~ 30 mg BN) and pressed with a force of 1 ton into a 5 mm in diameter pellet. This resulted in an edge jump of $\Delta\mu_x \sim 1.5$ at the Mo K-edge and $\Delta\mu_x \sim 0.2$ at the V K-edge. $H_5[PV_2Mo_{10}O_{40}] \cdot 13 H_2O$ was activated in 10 % propene in the temperature range from 300 K to 723 K. Extended XAS studies at the Mo K edge revealed the intact Keggin structure of the activated $H_5[PV_2Mo_{10}O_{40}] \cdot 13 H_2O$. Under isothermal reaction conditions (673 K, 698 K, and 723 K) the gas phase composition was rapidly changed from oxidizing (10 % propene and 10% oxygen in He) to reducing (10 % propene in He) reaction conditions.

X-ray absorption fine structure (XAFS) analysis was performed using the software WinXAS v3.1 [17] Background subtraction and normalization were carried out by fitting linear polynomials to the pre-edge and the post-edge region of the absorption spectra, respectively. The extended X-ray absorption fine structure (EXAFS) $\chi(k)$ was extracted by using cubic splines to obtain a smooth atomic background, $\mu_0(k)$. The pseudo radial distribution function $FT(\chi(k) \cdot k^3)$ was calculated by Fourier transforming the k^3 -weighted experimental $\chi(k)$ function, multiplied by a Bessel window, into the R space. EXAFS data analysis was performed using theoretical backscattering phases and amplitudes calculated with the ab-initio multiple-scattering code FEFF7. [18] Single scattering and multiple scattering paths in the Keggin ion model structure were calculated up to 6.0 Å with a lower limit of 2.0 % in amplitude with respect to the strongest backscattering path. EXAFS refinements were performed in R space simultaneously to magnitude and imaginary part of a Fourier transformed k^3 -weighted and k^1 -weighted experimental $\chi(k)$ using the standard EXAFS formula. [19] Structural parameters that are determined by a least-squares EXAFS refinement of a Keggin model structure to the experimental spectra are (i) one overall E_0 shift, (ii) Debye-Waller factors for single-scattering paths, (iii) distances of single-scattering paths, (iv) one third cumulant for the Mo – O or V – O distances in the first coordination shell and one third cumulant for all remaining scattering paths. Coordination numbers (CN) and S_0^2 were kept invariant in the refinement.

Results and discussion

The current manuscript consists of two parts. The first part establishes, that the structure of as-prepared $H_5[PV_2Mo_{10}O_{40}]$ and its structural evolution upon thermal activation is similar to that of $H_4[PVMo_{11}O_{40}]$ as described in Ref.14. $H_5[PV_2Mo_{10}O_{40}]$ was employed because the increased V content makes it more suitable for in situ XAS studies at the V K edge. The second part of the manuscript describes reversible changes in the local structure around the V centers and the correlation between the time-dependent evolution of the Mo average valence and the

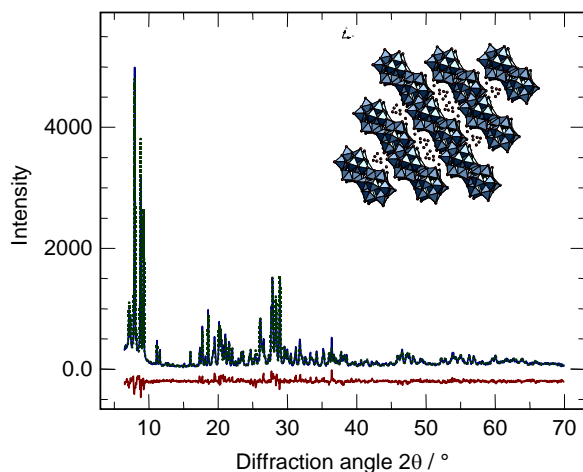


Figure 1: Experimental (dotted) and theoretical (solid) X-ray diffraction pattern of as-prepared $H_5[PV_2Mo_{10}O_{40}] \cdot 13 H_2O$ (P-1, $a = 14.03 \text{ \AA}$, $b = 14.17 \text{ \AA}$, $c = 13.59 \text{ \AA}$, $\alpha = 112.5^\circ$, $\beta = 109.8^\circ$, $\gamma = 60.5^\circ$). The inset shows a schematic structural representation of $H_5[PV_2Mo_{10}O_{40}] \cdot 13 H_2O$.

catalytic performance of material under rapidly changing reaction conditions (reducing and oxidizing).

Characterization and activation of as-prepared $H_5[PV_2Mo_{10}O_{40}] \cdot 13 H_2O$

Phase purity and a well-defined long-range order and local structure of the as-prepared $H_5[PV_2Mo_{10}O_{40}] \cdot 13 H_2O$ material were confirmed by XRD and XAS measurements. The experimental XRD pattern of the phase pure as-prepared $H_5[PV_2Mo_{10}O_{40}] \cdot 13 H_2O$ can be very well simulated with a calculated pattern of $H_3[PMo_{12}O_{40}] \cdot 13 H_2O$ [ICSD 31128] (Figure 1). This confirms, that the majority of V centers is located on regular Mo sites in the Keggin ions [14]. $H_5[PV_2Mo_{10}O_{40}] \cdot 13 H_2O$ was chosen to obtain an improved XAS signal at the V K edge. $H_5[PV_2Mo_{10}O_{40}] \cdot 13 H_2O$ exhibits a stability comparable to that of $H_4[PVMo_{11}O_{40}] \cdot 13 H_2O$ under the conditions employed. Conversely, a further increasing V content (V_3 and higher) results in a rapidly decreasing thermal stability of the corresponding polyoxomolybdate [20]. In good agreement with the XRD results, the local structure around the Mo and V centers in as-prepared $H_5[PV_2Mo_{10}O_{40}] \cdot 13 H_2O$ can be well described by assuming both metals on regular Mo sites in the Keggin ion (Figure 2 and Figure 3).

According to the procedure described in Ref. [14] the as-prepared $H_5[PV_2Mo_{10}O_{40}] \cdot 13 H_2O$ was activated by thermal treatment in 10 % propene in helium in the temperature range from 300 K to 723 K (rate of 5 K/min, dwell time of 10 min at 723 K). In situ XAFS measurements at the Mo K edge under steady-state reaction conditions yielded the local structure around the Mo centers in activated $H_5[PV_2Mo_{10}O_{40}]$. The local structure corresponded to the characteristically distorted Keggin structure previously reported (i.e. partially decomposed “lacunary” Keggin

ions). [14] XAFS data measured at the V K edge of activated $H_5[PV_2Mo_{10}O_{40}]$ under steady-state reaction conditions elucidate the geometric and electronic structure of the V centers in the real structure of the active catalyst. Because of the low photon energy of the V K edge, the required measuring time per spectrum did not permit time-resolved measurements.

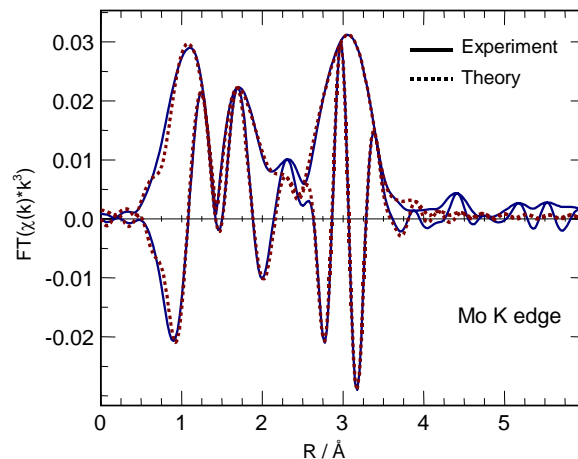


Figure 2: Experimental (solid) and theoretical (dashed) Mo K edge $FT(\chi(k) \cdot k^3)$ (not phase shift corrected) of as-prepared $H_5[PV_2Mo_{10}O_{40}] \cdot 13 H_2O$.

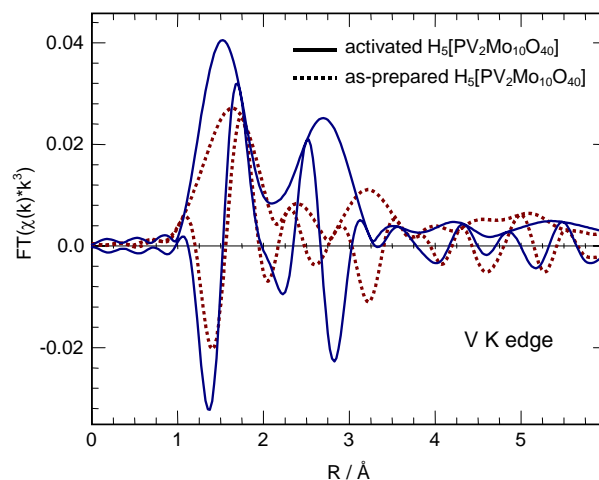


Figure 3: Experimental V K edge $FT(\chi(k) \cdot k^3)$ (not phase shift corrected) of as-prepared $H_5[PV_2Mo_{10}O_{40}] \cdot 13 H_2O$ (dashed) and activated $H_5[PV_2Mo_{10}O_{40}] \cdot 13 H_2O$ (solid).

Characterization of activated $H_5[PV_2Mo_{10}O_{40}]$ under reducing and oxidizing conditions

When switching the gas phase from reducing (propene) to oxidizing condition (propene and oxygen), evaluation of the characteristic pre-edge peak at the V K edge yielded an average valence that corresponded to 90 % V^{4+} and 10 % V^{5+} in the reduced state and 70 % V^{4+} and 30 % V^{5+} in the oxidized state. The average V valence was determined from the height of the pre-edge peak compared to

Table 1: Type and number (N) of atoms at distance R from the V center in the reduced and oxidized state of activated $\text{H}_5[\text{PV}_2\text{Mo}_{10}\text{O}_{40}] * 13 \text{H}_2\text{O}$ obtained from a refinement of a Keggin ion model structure (based on V in $\text{K}_2\text{H}[\text{PMo}_{12}\text{O}_{40}] * \text{H}_2\text{O}$, ICSD 209) to the experimental V K edge XAFS functions $\chi(k)$ (k range from 3.0 to 10 \AA^{-1} , R range from 0.9 to 4.0 \AA , E_0 (reduced) = 5.06 eV, E_0 (oxidized) = 7.49 eV, residual = 3.0, $N_{\text{ind}} = 16$, $N_{\text{free}} = 12$). The uncertainty in the distances amounts to about 0.03 \AA .

		Model			Oxidized state	
Type	N	R, (\AA)	R, (\AA)	σ^2 , (\AA^2)	R, (\AA)	σ^2 , (\AA^2)
V-O	1	1.71	1.56	0.0068	1.58	0.0126
V-O	2	1.91	1.97	0.0068	1.98	0.0126
V-O	2	1.92	1.97	0.0068	1.98	0.0126
V-O	1	2.46	2.40	0.0068	2.41	0.0126
V-Mo	0.6	-	2.84	0.0060	3.21	0.0091
V-Mo	2	3.42	3.52	0.0060	3.56	0.0091
V-P	1	3.57	3.49	0.0010	3.42	0.0011
V-Mo	2	3.72	3.72	0.0060	3.80	0.0091

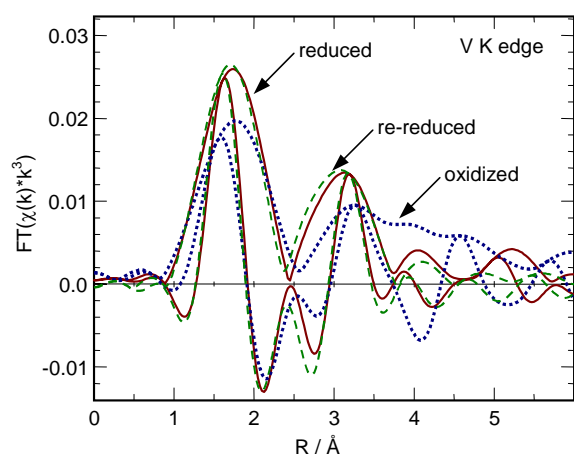


Figure 4: V K edge $\text{FT}(\chi(k) * k^3)$ (not phase shift corrected) of the V centers in activated $\text{H}_5[\text{PV}_2\text{Mo}_{10}\text{O}_{40}] * 13 \text{H}_2\text{O}$ in the reduced, oxidized, and re-reduced state.

reference samples (V_2O_5 , VO_2 , V_2O_3) according to Ref. [21]. The error bar in the absolute average valence amounts to about 0.03 [22] while even smaller changes obtained from time-resolved measurements can be analyzed reliably. An average V valence of less than 5+ in the oxidized state should be a prerequisite for the V centers to participate in the activation of gas phase oxygen and propene. Fully oxidized V and Mo centers would not possess vacant coordination sites to activate the gas phase reactants and, thus, would be catalytically inactive. Conversely, an average V valence between 5+ and 4+ reflects the dynamic behavior of the V valence during the catalytic cycle of propene oxidation.

The local structure around the V center in the reduced state of the activated $\text{H}_5[\text{PV}_2\text{Mo}_{10}\text{O}_{40}]$ catalyst corresponded to that of Mo sites in the Keggin ion with an additional short distance to one extra-Keggin Mo center. This structure is similar to that of V centers in the partially decomposed Keggin ion of activated $\text{H}_4[\text{PVMo}_{11}\text{O}_{40}]$. The latter has been described in detail in Ref. [14] Moreover, the vanadium centers in the lacunary Keggin ions exhibited

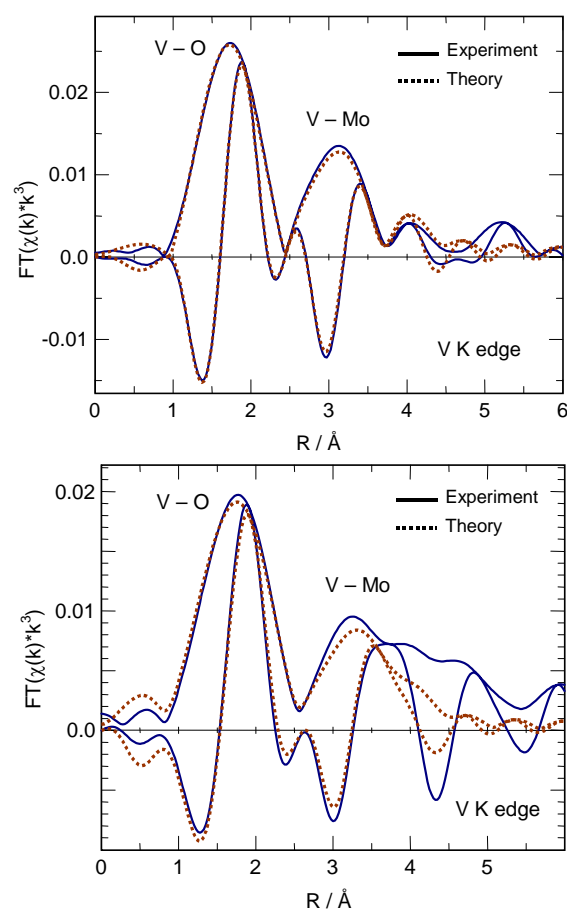


Figure 5: Theoretical (dashed) and experimental (solid) V K edge $\text{FT}(\chi(k) * k^3)$ (not phase shift corrected) of the reduced (A) and oxidized (B) state of the V centers in activated $\text{H}_5[\text{PV}_2\text{Mo}_{10}\text{O}_{40}] * 13 \text{H}_2\text{O}$.

a dynamic reversible behavior under changing reducing and oxidizing gas phase potential. (Figure 4) Upon switching from propene (reducing) to propene and oxygen (oxidizing) and back to propene, the local structure around the V center changed reversibly from a reduced state to an oxidized

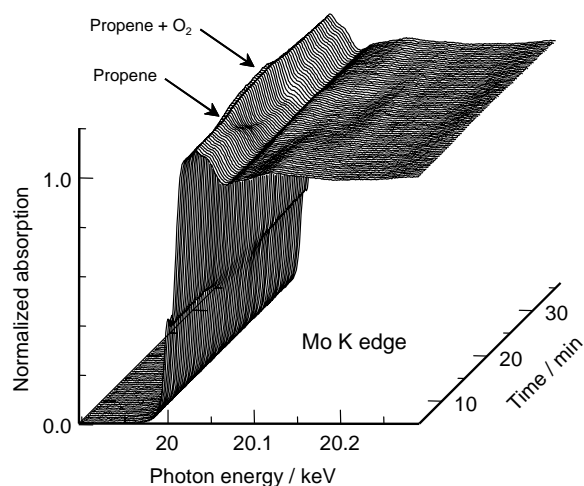


Figure 6: Evolution of Mo K edge XANES spectra of activated $H_5[PV_2Mo_{10}O_{40}] \cdot 13H_2O$ during isothermal switching of the gas phase from oxidizing conditions (propene/oxygen) to reducing conditions (propene) and back to oxidizing conditions.

state. While the reduced state is characterized by a short vanadium-molybdenum distance of about 2.8 Å, the oxidized state exhibits a longer distance of the vanadium center to the extra-Keggin Mo center of ~ 3.2 Å (Table 1, Figure 5A+B). The average V valence of less than 5+ and the significantly reduced amplitude of the $FT(\chi(k) \cdot k^3)$ of the vanadium centers in the oxidized state are indicative of a mixture of at least two sites exhibiting slightly different V-O distances around two different V centers (Table 1, Figure 5B).

Dynamic behavior of activated $H_5[PV_2Mo_{10}O_{40}]$ under reducing and oxidizing conditions

In addition to studies under steady-state conditions, time-resolved XAFS measurements at the Mo K edge were performed under changing reaction conditions (time-resolution of ~ 30 s/spectrum) (Figure 6). Therefore, the gas phase composition was isothermally switched from a reducing (propene) to an oxidizing (propene and oxygen) atmosphere (complete exchange in about 20 s in the in situ cell used). The time-resolved XAS investigations permitted to monitor the structural response of the catalyst on the changing reaction conditions. Analysis of the time-resolved XAS data revealed the solid-state kinetics of the bulk structural changes upon reduction and re-oxidation of the catalyst. The limited k range available at a sufficient time resolution did not permit a detailed EXAFS analysis of the rapid structural changes. Therefore, we focused on the near-edge region to determine the average Mo valence. The relative Mo K edge shift was converted into an average Mo valence according to the procedure reported in Ref. [23]. The evolution of the average Mo valence under reducing and oxidizing conditions at various temperatures is depicted in Figure 7. Upon switching from propene and oxygen to propene at 673 K, the average Mo valence exhibited

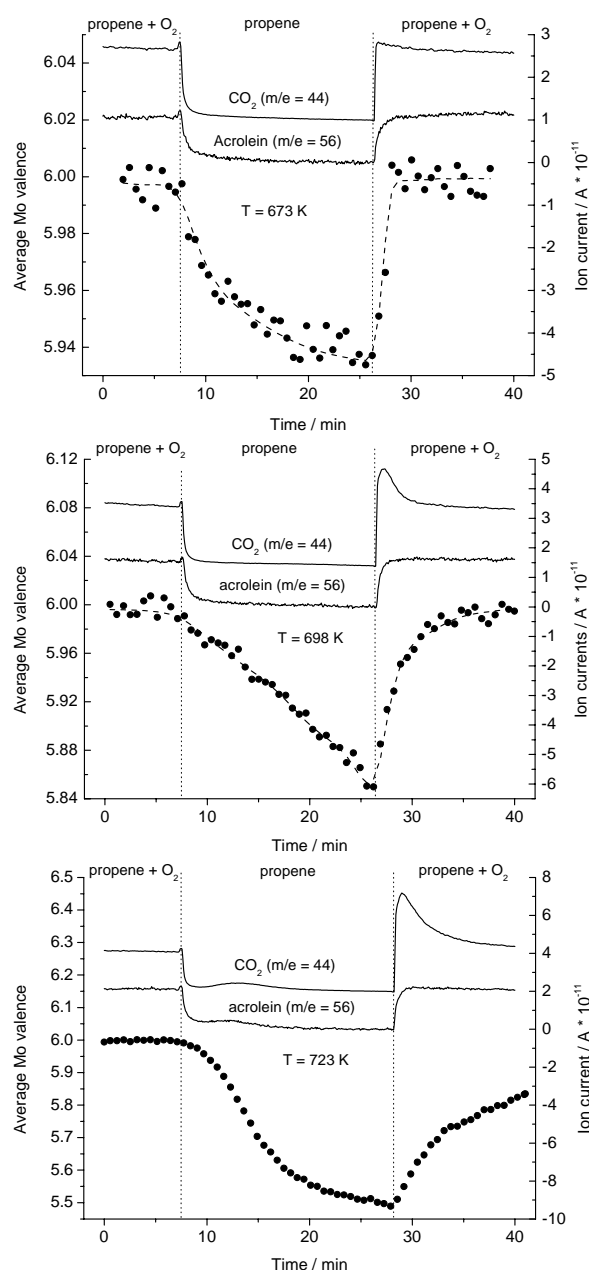


Figure 7: Evolution of Mo average valence of activated $H_5[PV_2Mo_{10}O_{40}] \cdot 13 H_2O$ during changing gas phase composition (propene to propene and oxygen) together with the corresponding evolution of acrolein and CO_2 in the gas phase at 673 K (A), 698 K (B), and 723 K (C).

a reduction from 6 to 5.94. Assuming spherical particles at a diameter of 100 Å (XRD), an average density of 4.3 g/cm³, a unit cell constant of the cubic Keggin structure of $a = 11.86$ Å, and about 1 Keggin ion per a^2 at the surface, reduction of one Mo^{6+} site to Mo^{5+} per surface Keggin ion results in a total average valence of ~ 5.94 . Apparently, at 673 K the reduction of the Mo centers in the lacunary Keggin ions is mostly limited to the surface of the accessible crystallites. Upon switching to oxidizing conditions (propene and oxygen) at 673 K, the mostly surface reduced catalyst was rapidly re-oxidized.

Under reducing conditions (propene), increasing the reaction temperature was accompanied by a more pro-

nounced decrease of the average valence of the Mo centers in the activated catalyst (Figure 7A+C). The more reduced catalyst at 723 K exhibited a prolonged re-oxidation behavior (Figure 7B). The corresponding extent of re-oxidation curve could be simulated with a solid-state kinetic model assuming three-dimensional diffusion to be the rate-limiting step (Figure 8). [23,24] An apparent activation energy of about 90 kJ/mol corroborated the assumption of oxygen diffusion limitation in the catalyst bulk.

Intriguingly, the selectivity of the catalyst at the various reaction temperatures exhibited a pronounced correlation with the degree of reduction and the solid-state kinetics of the re-oxidation process. After the reductive treatment in propene and switching back to propene and oxygen at 673 K, the rapid re-oxidation of the catalyst was accompanied by a rapid increase in the concentration of both acrolein and CO_2 in the gas phase (Figure 7A). This indicates that the entirely re-oxidized catalyst quickly regains its activity and selectivity in propene oxidation. Conversely, with increasing reaction temperature (698 K and 723 K, (Figure 7B+C)) the partially reduced catalyst exhibited a bulk-diffusion limited re-oxidation rate which coincides with an increased production of carbon dioxide and, hence, a reduced selectivity of the catalyst. The production of CO_2 decreased with the increasing re-oxidation of the catalyst and, after complete re-oxidation, reached the same activity and selectivity as prior to the switching experiments.

The impact of the partially reduced state of the activated $\text{H}_5[\text{PV}_2\text{Mo}_{10}\text{O}_{40}]$ catalyst on the selectivity is schematically illustrated in Figure 9. The lower average valence detected during slow re-oxidation of the catalyst corresponds to a larger number of $\text{V}^{4+}\text{-Mo}^{5+}$ sites and oxygen vacancies (Figure 9, right side). According to the XAFS data under steady-state conditions, these $\text{V}^{4+}\text{-Mo}^{5+}$ sites possess the characteristic short metal – metal bond of the reduced state of the activated $\text{H}_5[\text{PV}_2\text{Mo}_{10}\text{O}_{40}]$ catalyst (Figure 4, Figure 9, (A)). Moreover, these $\text{V}^{4+}\text{-Mo}^{5+}$ sites may be particularly effective in activating gas phase oxygen, which results in an over-supply of surface-bound electrophilic oxygen. This electrophilic oxygen is prone to further oxidize propene or acrolein to CO_2 and water [25 and references therein] (Figure 9, (B)). Upon complete re-oxidation of the catalyst, the density of these over-active sites decreases (Figure 9, left). $\text{V}^{4+}\text{-Mo}^{6+}$ sites that exhibit a longer metal-metal distance and a lower tendency to form electrophilic oxygen species govern the catalytic performance. Hence, adsorbed propene is mostly oxidized to acrolein by nucleophilic lattice oxygen, and the selectivity of the catalyst increases (Figure 9, (C)).

The correlation between electronic structure and catalytic performance corroborates the assumption, that the selectivity of the catalyst is governed by the electronic structure of the surface. The latter in turn appears to be determined by the electronic defect structure of the underlying bulk. [25] For the activated $\text{H}_5[\text{PV}_2\text{Mo}_{10}\text{O}_{40}]$ catalyst studied, reaction conditions that favor a conventional redox mechanism with fast reduction and diffusion-limited re-oxidation lead to low selectivity. Conversely, reaction con-

ditions that maintain a rapid re-oxidation and a small amount of Mo^{5+} centers in the catalyst result in an increased selectivity. Hence, it may be concluded that in a process that involves diffusion of oxygen ions in the catalyst bulk and a prolonged lifetime of partially reduced $\text{V}^{4+}\text{-Mo}^{5+}$ metal sites, total oxidation of propene will dominate. On the other hand, catalytic oxidation of propene proceeding on an oxidized $\text{V}^{4+}\text{-Mo}^{6+}$ active site at the surface of the catalyst yields an improved selectivity towards partial oxidation products.

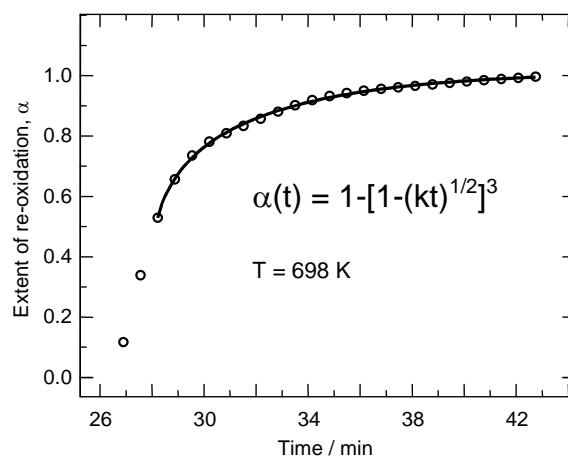


Figure 8: Refinement of a solid-state kinetic model for three-dimensional solid-state diffusion ($\alpha(t) = 1 - [1 - (kt)^{1/2}]^3$) to the experimental extent of re-oxidation of activated $\text{H}_5[\text{PV}_2\text{Mo}_{10}\text{O}_{40}] * 13 \text{H}_2\text{O}$ at 698 K (Figure 3B).

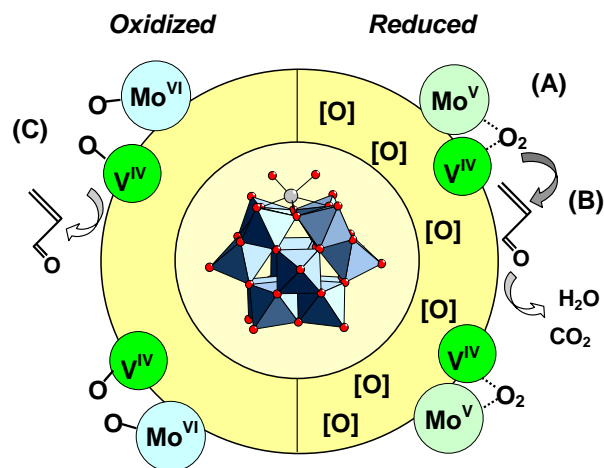


Figure 9: Schematic representation of the Mo – V local structure of the active site in the reduced ($\text{V}^{4+}\text{-Mo}^{5+}$, right) and oxidized ($\text{V}^{4+}\text{-Mo}^{6+}$, left) state of activated $\text{H}_5[\text{PV}_2\text{Mo}_{10}\text{O}_{40}] * 13 \text{H}_2\text{O}$ in partial oxidation of propene. (A) Electrophilic oxygen species activated by $\text{V}^{4+}\text{-Mo}^{5+}$ site (right) which (B) result in total oxidation of propene (right). (C) Nucleophilic lattice oxygen on $\text{V}^{4+}\text{-Mo}^{6+}$ site (left) favoring selective oxidation. [O] denote oxygen vacancies in the bulk (right)

Conclusions

The time-resolved in situ structural investigations described here yielded an intriguing correlation between the average valence of the Mo centers in a partial oxidation catalyst, the solid-state kinetics of the re-oxidation behavior of the catalyst under dynamic conditions, and the catalytic selectivity. Apparently, the electronic structure of the bulk and of the surface of the catalyst change dynamically under the reaction conditions employed and, thereby, determines the catalytic selectivity of the surface. Moreover, the local structure around the V centers in the proposed active site also exhibits a dynamic behavior as a function of the reduction potential of the gas phase. Correlations between the selectivity of a metal oxide catalyst in partial oxidation reactions and the electronic structure of the corresponding metal centers have been previously proposed based on

model assumptions [25]. However, experimental data that corroborate these assumptions remain scarce. It emerges, that time-resolved bulk structural studies under changing reaction conditions are indeed capable of further elucidating correlations between the dynamic structural behavior of a heterogeneous catalyst and catalytic properties that are not readily available from investigations under steady state conditions.

Acknowledgement

The *Hamburger Synchrotronstrahlungslabor*, HASYLAB, is acknowledged for providing beamtime for this work.

References

- [1] B.L. Knip, T. Ressler, A. Rabis, F. Girgsdies, M. Baenitz, F. Steglich, R. Schlögl, *Angewandte Chemie Int. Ed.* **2004**, 43, 112–115.
- [2] F.W.H. Kampers, T.M.J. Maas, J. van Grondelle, P. Brinkgreve, D.C. Koningsberger, *Rev. Sci. Instrum.* **1989**, 60, 2635.
- [3] G. Meitzner, S.R. Bare, D. Parker, H. Woo, D.A. Fischer, *Rev. Sci. Instrum.* **1998**, 69, 2618.
- [4] B.S. Clausen, K. Graback, G. Steffensen, P.L. Hanssen, H. Topsøe, *Catal. Lett.* **1993**, 20, 23.
- [5] G. Sankar, J.M. Thomas, *Topics in Catalysis* **1999**, 8, 1.
- [6] J.D. Grunwaldt, L. Basini, and B.S. Clausen, *J. Catal.* **2001**, 200, 321.
- [7] B.M. Weckhuysen, Ed., *In-situ Spectroscopy of Catalysts*, American Scientific Publishers, Los Angeles, USA **2004** and references therein.
- [8] M.M. Lin, *Appl. Catal. A: General* **2001**, 207, 1–16.
- [9] T. Okuhara, N. Mizuno, M. Misono, *Advances in Catalysis* **2001**, 41, 443-673.
- [10] M.E. Davis, C.J. Dillon, J.H. Holles, J. Labinger, *Angewandte Chemie Int. Ed.* 2002, 41, 858-860.
- [11] J.H. Holles, C.J. Dillon, J.A. Labinger, M.E. Davis, *J. Catal.* **2003**, 218, 42–53;
- [12] J.H. Holles, C.J. Dillon, J.A. Labinger, M.E. Davis, *J. Catal.* **2003**, 218, 54–66.
- [13] J. Wienold, O. Timpe, T. Ressler, *Chemistry, A European Journal* **2003**, 9, 6007–6017.
- [14] T. Ressler, O. Timpe, F. Girgsdies, J. Wienold, T. Neisius, *J. Catal.* **2005**, 231, 279–291.
- [15] S. Berndt, D. Herein, F. Zemlin, E. Beckmann, G. Weinberg, J. Schütze, G. Mestl, R. Schlögl, *Ber. Bunsenges. Phys. Chem.* **1998**, 102, 763.
- [16] G. A. Tsigdinos, *Topics in Current Chemistry* **1987**, 76, 1-64.
- [17] T. Ressler, *J. Synch. Rad.* **1998**, 5, 118.
- [18] J.J. Rehr, C.H. Booth, F. Bridges, S.I. Zabinsky, *Phys. Rev. B* **1994**, 49, 12347.
- [19] T. Ressler, S.L. Brock, J. Wong, S.L. Suib, *J. Phys. Chem. B* **1999**, 103, 6407–6420.
- [20] O. Timpe, personal communication.
- [21] J. Wong, F.W. Lytle, R.P. Messmer, D.H. Maylotte, *Phys. Rev. B* **1984**, 30, 5596.
- [22] R.E. Jentoft, A.H.P. Hahn, F.C. Jentoft, T. Ressler, *Phys. Chem. Chem. Phys.* **2005**, 7, 2830.
- [23] T. Ressler, R.E. Jentoft, J. Wienold, T. Neisius, *J. Catal.* **2002**, 210, 67–83.
- [24] C.H. Bamford, Ed., “Comprehensive Chemical Kinetics”, Vol. 2, Elsevier 1968.
- [25] G. Centi, F. Canani, F. Trifiro, “Selective Oxidation by Heterogeneous Catalysis”, *Fundamental and Applied Catalysis*, Eds. M.V. Twigg, M.S. Spencer, Kluwer Academic / Plenum Publishers, New York 2001.